Volume 58(12): 1083–1092, 2010
Journal of Histochemistry & Cytochemistry
http://www.jhc.org

ARTICLE

Differential Endothelial Gap Junction Expression in Venous Vessels Exposed to Different Hemodynamics

Chi-Jen Chang, Lung-Sheng Wu, Lung-An Hsu, Gwo-Jyh Chang, Chin-Fen Chen, Hung-I Yeh, and Yu-Shien Ko

The First Cardiovascular Division, Chang Gung Memorial Hospital (C-JC,L-SW,L-AH,C-FC,Y-SK) and Graduate Institute of Clinical Medical Sciences (G-JC), Chang Gung University, Tao-Yuan, Taiwan, and Department of Internal Medicine, Mackay Memorial Hospital, Mackay Medical Collage, Taipei, Taiwan (H-IY)

SUMMARY After being anastomosed with the artery, vein graft is exposed to abruptly increased hemodynamic stresses. These hemodynamic stresses may change the profile of endothelial gap junction expression as demonstrated in the artery, which may subsequently play active roles in physiological adaptation or pathophysiological changes of the vein grafts. We investigated the endothelial expression of gap junction in the venous vessels exposed to different hemodynamic stresses. Immunocytochemical analysis of the endothelial Cx expression was performed by observing the whole mounts of inferior vena cava (IVC) of aortocaval fistula (ACF) rats or IVC-banded ACF rats using confocal microscope. Immunocytochemical analysis demonstrated that in the endothelium of the native vein, the gap-junctional spot numbers (GJSNs) and the total gap-junctional areas (TGJAs) of Cx40 and Cx43 were lower than those of the thoracic aorta and that Cx37 was hardly detectable. In the IVCs of ACF rats, which were demonstrated to be exposed to a hemodynamic condition of high flow velocity and low pressure, the GJSNs and the TGJAs of all three Cxs were increased. In the IVCs of IVC-banded ACF rats, which were exposed to a hemodynamic condition of high pressure and low flow velocity, the GJSNs and the TGJAs of Cx37 increased markedly and those of Cx40 and Cx43 remained without significant changes. In conclusion, the endothelial expressions of gap junctions in the native veins were lower than those of the arteries. When exposed to different hemodynamic stresses, the gap junctions were expressed in specific patterns. **(J Histochem Cytochem 58:1083–1092, 2010)**

KEY WORDS
gap junction
hemodynamic stress
vein

In uremic patients, the superficial vein is the most common vessel used for the creation of arteriovenous fistulas for hemodialysis access. The superficial vein also remained the major conduit for bypass surgery in patients with coronary or peripheral arterial diseases. After being anastomosed with the artery, the venous vessel is exposed to various abruptly increased hemodynamic stresses, including increased flow (Greenfield et al. 1972), laminar (Jiang et al. 2004) and oscillatory shear stresses (Wang et al. 1990), intraluminal pressure (Spray and Roberts 1976), and cyclic circumferential strain (Casey et al. 2001). The endothelial expression of Cxs, the component proteins of gap junctions, has been demonstrated to be regulated by the hemodynamic stresses in the arteries (Gabriels and Paul 1998). However, the baseline Cx expression and the changes in Cx expression when exposed to arterialized hemodynamics in venous vessels remain to be elucidated. It is essential to clarify these gap junction expression profiles because the gap junctions may play important roles in regulating vascular tone acutely, in remodeling of vascular structure, and even in the development of neointimal hyperplasia after being anastomosed with the arteries.

Correspondence to: Yu-Shien Ko, MD, PhD, The First Cardiovascular Division, Chang Gung Memorial Hospital, 5 Fu-Hsing St., Kuei-Shan, Tao-Yuan, Taiwan. E-mail: c12037@adm.cgmh.org.tw

Received for publication April 13, 2010; accepted August 18, 2010 [DOI: 10.1369/jhc.2010.956425].

Accordingly, we investigated the Cx expression in the luminal endothelial cells of inferior vena cava (IVC) of the rat with aortocaval fistula (ACF) or with IVC-banded ACF. Endothelial Cx expression was observed in the whole mounts of IVC using ICC.

Materials and Methods

Rat Model of ACF

The ACF model was created in adult male Sprague–Dawley rats (300–350 g) as described previously (Nath et al. 2003). After anesthetization with ketamine (0.2 ml/100 mg IP), the abdominal cavity was opened. The IVC and aorta (Ao) were exposed and clamped right below the renal artery proximally and right above the iliac bifurcation distally. An 18-gauge needle was used to puncture the lateral wall of the abdominal Ao, right superior to the distal clamped site. The needle was advanced to cross the opposite aortic wall toward the IVC and then penetrated the neighboring wall of the IVC cautiously to create a hole connecting both lumens of the abdominal Ao and the IVC. The procedure was done cautiously to avoid puncturing the opposite wall of the IVC. Finally, the needle was withdrawn gently; the entry point was sealed with cyanoacrylate glue (Vetbond 3M; St. Paul, MN). The patency of fistula was confirmed by pulsation and color change in the IVC, resulting from the shunt of oxygenated blood from the Ao. For creation of the IVC-banded ACF rats, the ACF was created first as described earlier. A 2-0 silk suture was then snared around the IVC right below the renal artery. Then an 18-gauge needle was placed next to the IVC and the suture was snugly tied around the needle and vessel. After ligation, the needle was removed. To test the potential effect of simple banding of IVC on the endothelial Cx expression, a model of IVC banding without ACF was created. The IVC was banded as was done in the rats with IVC-banded ACF. Sham operations were done as in the procedure of ACF creation except that the needle used to puncture the lateral wall of the Ao was not advanced to cross the wall opposite to the entry site.

All the animal experiments were performed according to the guidelines of the Committee on Animal Research at Chang Gung Memorial Hospital.

Duplex Scan to Assay IVC Flow

Duplex scans (Acuson; Aspen, Willoughby, OH) were performed to assay flow patterns and velocity of IVC. B-mode and Doppler imaging was obtained using a high-resolution linear transducer at a frequency of 15 MHz. After euthanization, laparotomy was done and the IVC was exposed. The transducer was then placed over the IVC as lightly as possible to avoid compression of the vessel, as guided by the B-mode image. The IVC flow velocity was recorded along the entire IVC segment.

Measurement of IVC Pressure

For measurement of IVC pressure, an 18-Fr intravenous catheter needle was inserted into the IVC with an entry site lower to the AV anastomosis. The cannula was connected to a pressure transducer (MLT0380/D; ADInstruments, Castle Hill, Australia), and the signals were amplified by a bridge amplifier (QuadBridge Amp; ADInstruments). Signals from these amplifiers were digitized at 4 kHz using a PowerLab/4sp A/D converter (ADInstruments) and stored in an online computer. The data were analyzed by Chart 5.4.2 software (ADInstruments).

Tissue Preparation

IVCs were harvested 1 week after surgery. The specimens were harvested with the animals perfusion fixed with 3% paraformaldehyde in PBS at 100 mm Hg for 10 min. The adventitia of the IVCs was trimmed gently to avoid vessel injury before perfusion fixation. After perfusion fixation, the IVCs were harvested and the specimens were transected through the midlevel into the upper and lower segments. The vessel was opened longitudinally, and the whole tissue was submitted for IHC study. Adequate tissue preservation during processing of IVC specimens has been verified in a previous study by our group (Chang et al. 2009). Immunolabeling using an anti-CD31 antibody as an endothelial cell marker was done in the IVC specimens of all groups for further verification of luminal endothelium preservation. Anti-CD31 signals were constantly found in all IVC specimens throughout the luminal surface except at the edge, which confirmed the adequate preservation of endothelial cells (data not shown).

Immunofluorescence Labeling and Confocal Microscopic Study of Gap-junctional Connexins

Because Cx37, Cx40, and Cx43 have been demonstrated to be the major Cxs expressed in vascular endothelial cells in mammals (Van Rijen et al. 1997; Yeh et al. 1998) and anti-Cx45 signal was not detectable in the endothelium of IVC in a preliminary IHC study (data not shown), anti-Cx37, anti-Cx40, and anti-Cx43 antibodies were used for the immunohistochemical reaction to investigate the Cx expression profile. The polyclonal antisera against Cx37 or Cx40 were produced in rabbits against the synthetic peptides corresponding to residues 266–281 or 256–270 of the cytoplasmic C-terminal tail of rat Cx37 or Cx40, respectively, as validated in previous studies (Yeh et al. 1998,2000,2003). For Cx43 and CD31 immunolabeling, a monoclonal mouse anti-rat Cx43 antibody (BD Transduction Laboratories; San Jose, CA) and a goat-anti-mouse CD31 antibody (Santa Cruz; Santa Cruz, CA) were used. For the immunohistochemical reaction, the perfusion-fixed IVC samples were first rinsed in PBS for 5 min and blocked in 0.5% BSA in PBS for 15 min.

The samples were incubated with anti-Cx37 (1:500 at 4C overnight), anti-Cx40 (1:1000 at 4C overnight), anti-Cx43 (1:500 at room temperature for 1 hr), or anti-CD31 (1:500 at 4C overnight) and then with appropriate CY3-conjugated secondary bodies at room temperature for 1 hr. During the immunolabeling process, all steps were performed in 2-ml Eppendorf tubes to prevent injury to the endothelial surface. After immunoreactions, the IVC tissues were carefully placed on slides with the luminal side facing up and mounted using Citifluor mounting medium (Agar Scientific; Mannheim, Germany). The signals of anti-Cx labeling in the luminal EC of specimens were then examined using a confocal laser scanning microscope (Leica TCS

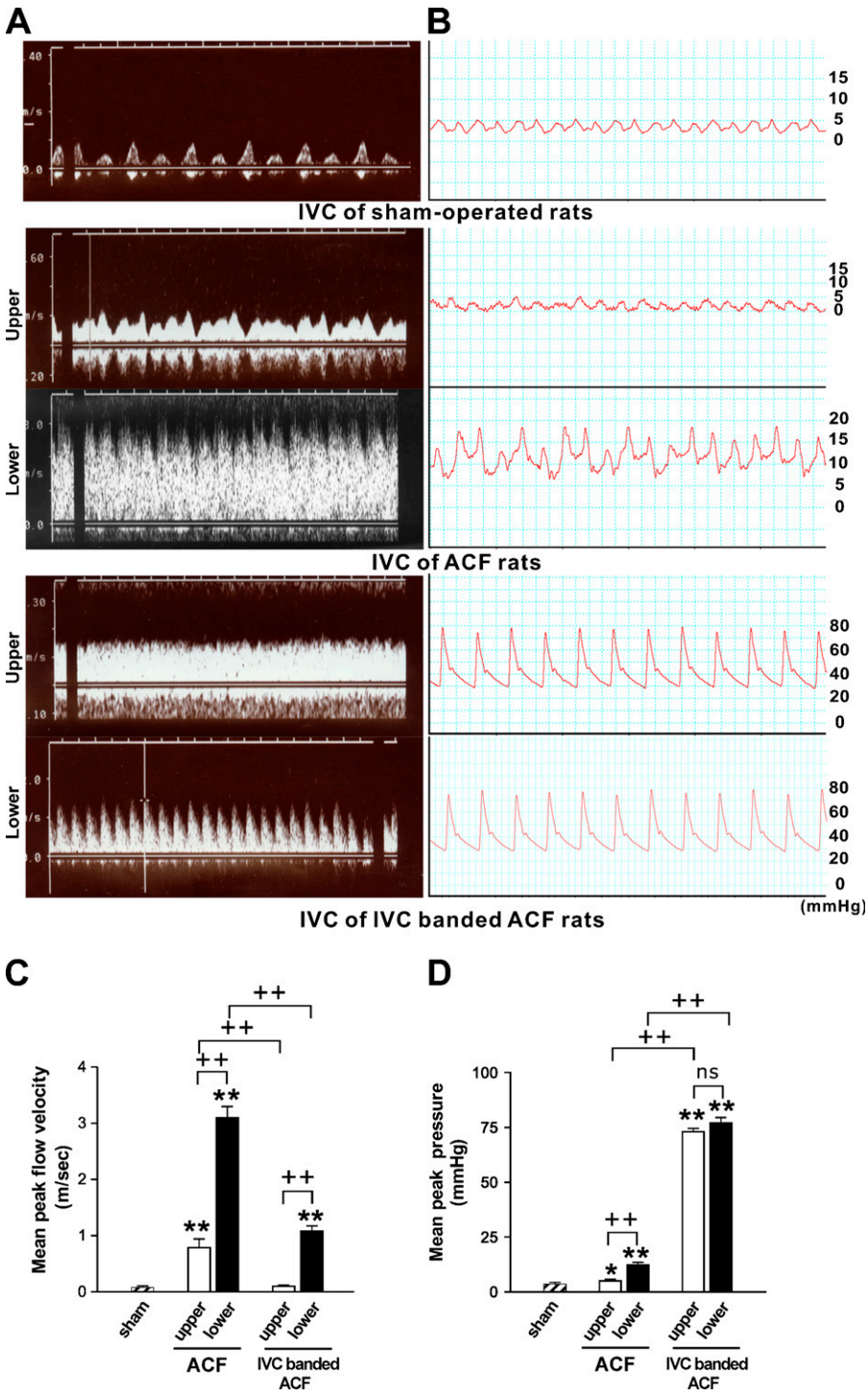

Figure 1 Hemodynamic assays for inferior vena cava (IVC) of sham-operated, aortocaval fistula (ACF), and IVC-banded ACF rats (n=3 for each group). (**A**) Duplex scan assay to detect the flow of IVC. (**B**) Pressure tracing of IVC. (**C**) Bar graph of the mean peak flow velocity of IVC. (**D**) Bar graph of the mean peak pressure of IVC. **p<0.001 when compared with sham; +p<0.05, ++p<0.001, and nonsignificant (ns) difference when compared between two indicated groups.

SP; Stansted, UK). The images were observed at a magnification of ×630. Each recorded image was 1024 × 1024 pixels in size, and projection views of consecutive optical sections were taken at 0.6-μm intervals throughout the full thickness of the endothelial signals. Each pixel represented 0.23 μm. All specimens were examined within 24 hr of immunolabeling. For each specimen, five images were randomly selected and analyzed using QWIN image analysis software (Leica) with the setting kept constant throughout the analysis. Mean values (±SDs) of the number of immunolabeled gap junctions per 100 μm^2 of luminal surface area and the total area of immunolabeled gap junction expressed as the percentage of luminal surface area were obtained for each experimental group. The immunoconfocal method has been well established in previous studies to provide reliable data about the relative level of a given Cx assembled in the form of gap junctions, although it does not provide data of the absolute amount of Cxs (Green et al. 1993; Blackburn et al. 1995; Yeh et al. 1997).

Statistical Analysis

Data were presented as mean ± SD. Differences between two groups were determined by Student's *t*-test. For multiple groups, one-way ANOVA with post hoc Scheffe test was used to compare data among groups. p Value <0.05 was considered statistically significant.

Results

Hemodynamic Study

IVC flow was observed using the duplex scan at 1 week ($n=3$ for each group) as demonstrated in Figure 1A. In the sham-operated rats, a normal central venous flow pattern, reflecting atrial pulsation, was detected. The flow velocity was low and constant throughout the entire IVC segment. In the ACF rats, a flow of broad velocity spectrum was detected in the IVCs, indicating a turbulent flow. The flow was pulsatile with a highly increased velocity at the lower IVC segment and remained pulsatile but with a lower velocity at the upper IVC segment. When compared between the lower and upper IVC, the mean peak velocity was significantly higher in the former ($p<0.001$), and the mean peak velocity of both was significantly higher than that of the sham-operated rats ($p<0.001$ for both). In the IVC-banded ACF rats, a pulsatile and turbulent flow was detected in the lower IVC and a continuous flow

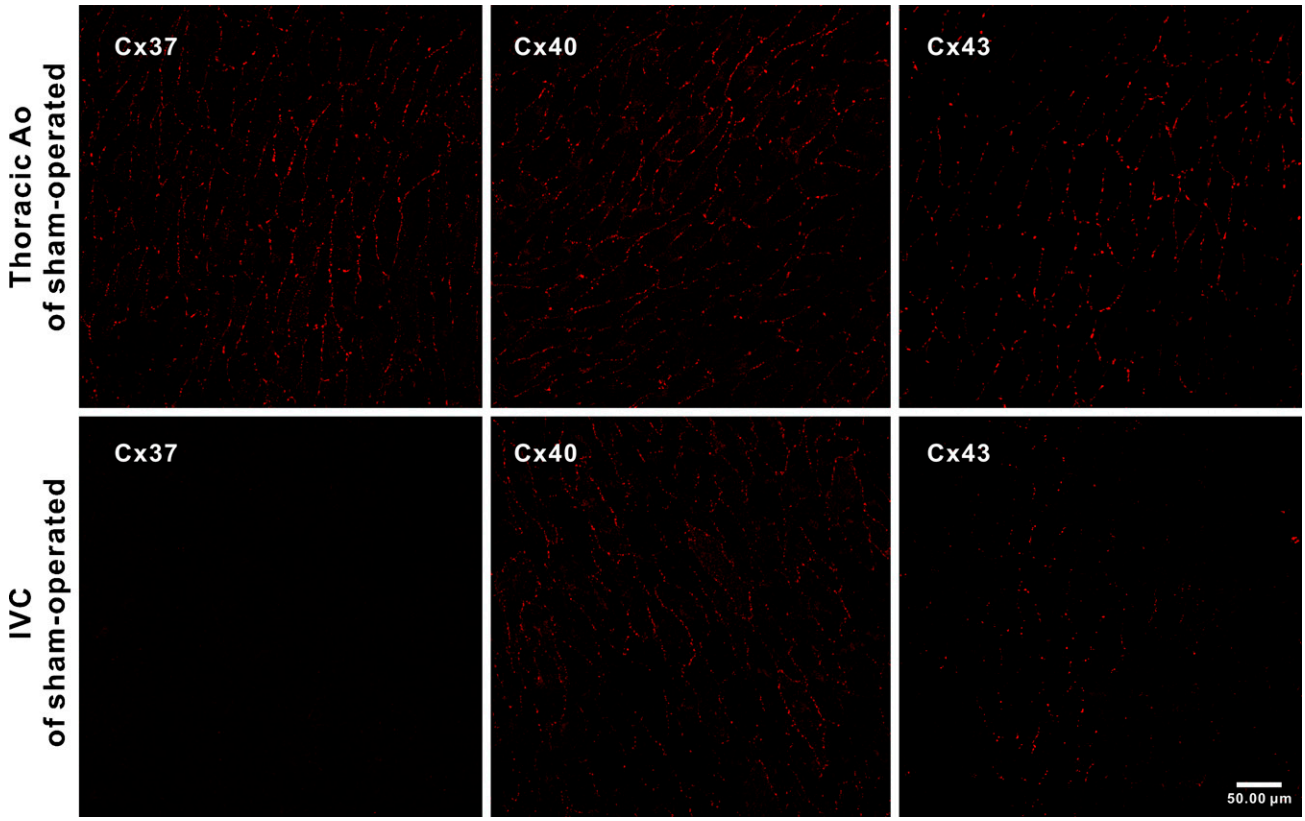

Figure 2 Representative en face confocal images showing the expression of Cx37, Cx40, and Cx43 in endothelium of the thoracic aorta (Tho Ao) and IVC ($n=4$ for each).

was detected in the upper IVC. In the lower IVC, the mean peak flow velocity was significantly higher than that of the IVC of sham-operated rats ($p<0.001$) and was significantly lower than that of the corresponding segment of ACF rats ($p<0.001$). In the upper IVC, the mean peak velocity was similar to that of the IVC of sham-operated rats ($p=0.146$) and was significantly lower than that of the corresponding IVC segment of ACF rats ($p<0.001$).

The pressure tracing of the IVC was performed at 1 week ($n=3$ for each group) as demonstrated in Figure 1B. In the sham-operated rats, the pressure tracing of IVC showed a normal central venous pressure waveform. The pressure was low and constant throughout the whole segment. In the ACF group, the IVC pressure was pulsatile and the level declined from the aortocaval junction upward toward the heart. The mean peak pressures in both the upper and lower IVC were significantly higher than that of the sham-operated rats ($p=0.010$ and $p<0.001$, respectively). When comparing the lower and upper segments, the mean peak pressure in the lower segment was significantly higher ($p<0.001$). In the IVC-banded ACF rats, the pressures of the lower and upper IVC were significantly higher than those of the corresponding segments of the ACF rats and also higher than that of the sham-operated rats ($p<0.001$ for all). The quantitative data of the hemodynamic study are summarized in Figures 1C and 1D. These findings confirmed that the ACF rats represent a vein graft model of high flow velocity and mildly but significantly increased pressure and IVC-banded ACF rats represent a model of high pressure and relatively low flow velocity.

Endothelial Cx Expression in Thoracic Ao and IVC of Sham-operated Rats

The specimens of IVC and thoracic Ao of sham-operated rats ($n=4$ for each group) immunoreacted with anti-Cx37, anti-Cx40, and anti-Cx43 antibodies were observed en face by confocal microscopy. Punctuated anti-Cx signals were found to delineate the cell borders of luminal endothelial cells of either IVCs or thoracic Aos with the same pattern as that found in a previous study (Yeh et al. 1998). In the thoracic Ao, the anti-Cx37, anti-Cx40, and anti-Cx43 signals were all diffusely distributed. In IVCs of the sham-operated rats, the anti-Cx40 signals were found to be the prevailing isoform and were present in most of the endothelial cells with variable abundance. Different from the diffuse distribution of Cx43 in the normal thoracic Ao, the anti-Cx43 signals were localized to sparsely scattered patches throughout the entire IVC segment. The patches were composed of tens of endothelial cells. The anti-Cx37 signals were hardly detectable throughout the entire IVC (Figure 2). Quantitative analysis showed that the gap-junctional spot numbers (GJSNs) and total gap-junctional areas (TGJAs) of Cx37, Cx40, and Cx43 were significantly lower in the IVC when compared with those of the thoracic Ao ($p<0.001$ and $p=0.001$ for Cx37, $p=0.001$ and $p<0.001$ for Cx40, and $p<0.001$ and $p<0.001$ for Cx43) (Figure 3).

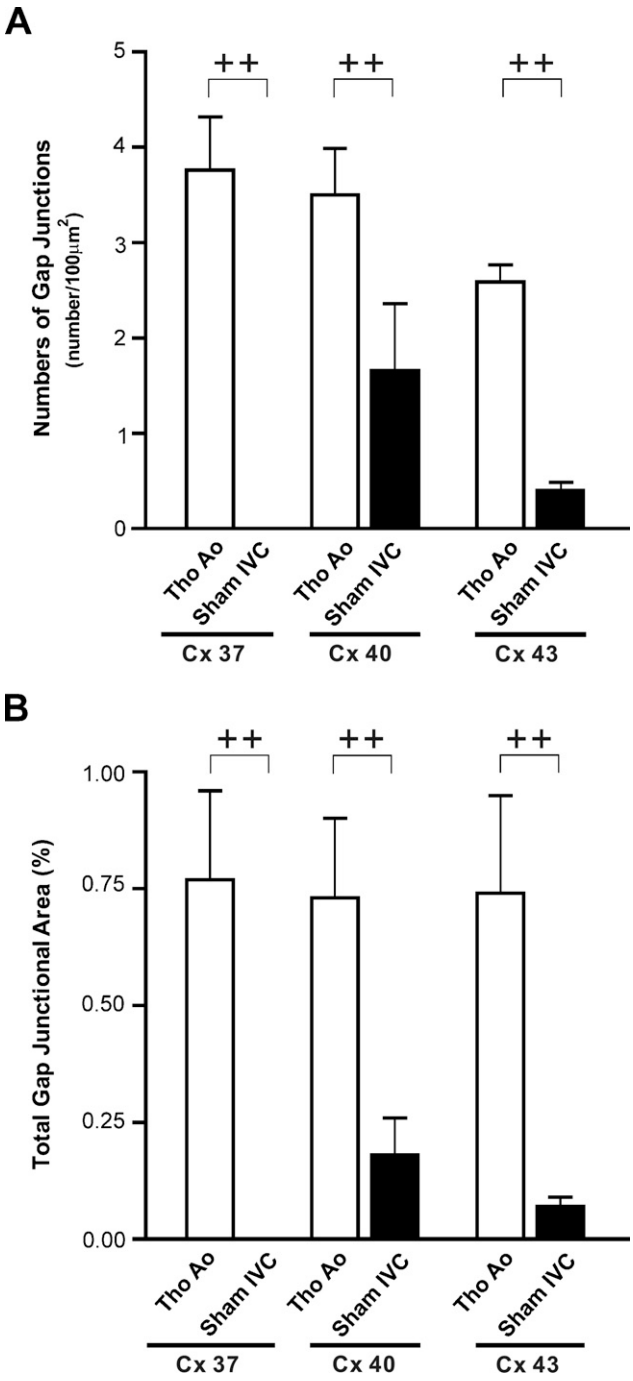

Figure 3 Immunoconfocal analysis of gap junction spots of endothelium of Tho Ao and IVC of sham-operated rats ($n=4$ for each) detected by antibodies against Cx37, Cx40, and Cx43. (**A**) Gap-junctional spot numbers (GJSNs). (**B**) Total gap-junctional areas (TGJAs). $++p<0.001$ when compared between two indicated groups.

The Journal of Histochemistry & Cytochemistry

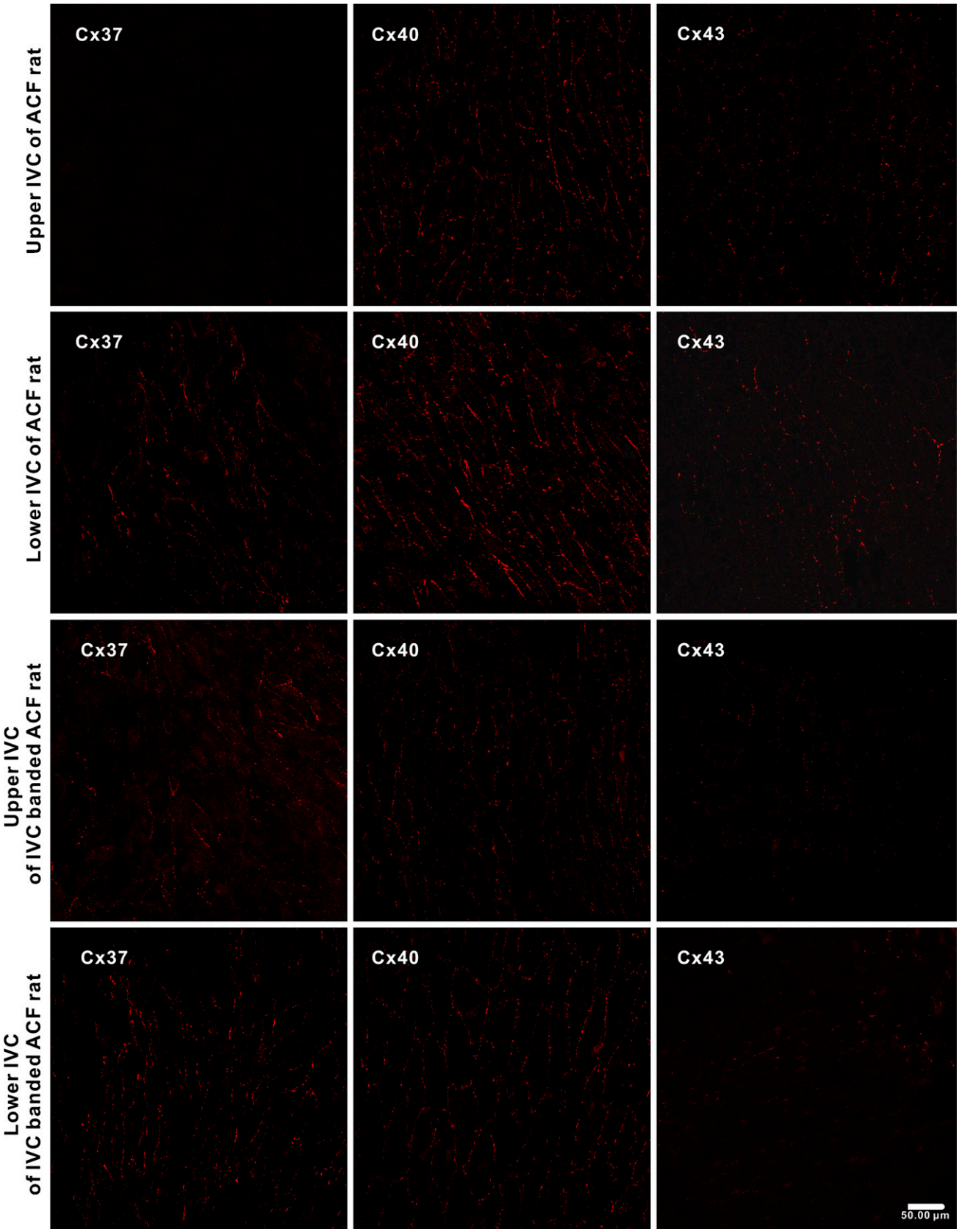

Endothelial Cx Expression in IVC of ACF Rats

Endothelial Cx expressions in the IVC of ACF rats were investigated 1 week after operation (n=4). As the hemodynamic study showed significant difference in flow velocity and pressure between the upper and lower IVC, the Cx expression in both segments was observed separately. In the upper IVC of ACF rats, the anti-Cx40 and anti-Cx43 signals were distributed in a pattern similar to that found in IVCs of the sham-operated rats, and Cx37 remained undetectable. In the lower IVC, the abundance of Cx40 was increased in general, but was more heterogenous. The Cx43 was distributed as isolated patches as found in the IVC of sham-operated rats. However, the patches with positive anti-Cx43 labeling were generally larger and were composed of tens to hundreds of cells. Different from the IVCs of the sham-operated rats, small patches of positive anti-Cx37 signals appeared in the lower IVC of the ACF rats (Figure 4). Quantitative analysis showed that the GJSNs and TGJAs of Cx37, Cx40, and Cx43 in the upper IVCs of ACF rats were similar to those in the IVCs of sham-operated rats (p=1.0 and 1.0 for Cx37, p=0.618 and 0.851 for Cx40, and p=0.476 and 0.966 for Cx43). In contrast, the GJSNs and the TGJAs of all three Cxs in the lower IVCs of ACF rats were significantly higher when compared with those in the IVCs of the sham-operated rats (p<0.001 and p=0.002 for Cx37, p<0.001 and p<0.001 for Cx40, and p=0.001 and p=0.001 for Cx43). When compared between the upper and lower IVC, the GJSNs and TGJAs of all three Cxs were significantly higher in the latter (p=0.011 and p=0.002 for Cx37, p<0.001 and p<0.001 for Cx40, and p=0.001 and p=0.010 for Cx43) (Figure 5).

Endothelial Cx Expression in IVC of IVC-banded ACF Rats

In the IVC-banded ACF rats, the signals of all three Cxs were found in both the lower and upper segments. Instead of small patches in the lower IVCs of ACF rats, the anti-Cx37 signals were distributed in large patches composed of hundreds of cells in the lower IVCs of IVC-banded ACF rats. In the upper IVCs, the anti-Cx37 signals were distributed in small patches. The distribution patterns of Cx40 and Cx43 were similar to those of the sham-operated rats (Figure 4). Quantitative analysis showed that the GJSN and TGJA of Cx37 of both the upper and lower IVCs were significantly higher than those of the sham-operated rats (upper IVC vs sham-operated: p=0.008 and p=0.014; lower IVC vs sham-operated: p<0.001 and p<0.001). When comparing the upper and lower IVCs of the IVC-banded ACF rats, the GJSN and TGJA of the former were significantly lower (p=0.001 and p=0.002). In contrast, the GJSNs and TGJAs of the Cx40 and Cx43 in both the upper and lower IVCs of IVC-banded ACF rats were similar to those of the IVCs of sham-operated rats (upper IVC vs sham-operated: p=0.968 and p=0.999 for Cx40 and p=1.000 and p=0.998 for Cx43; lower IVC vs sham-operated: p=0.968 and p=0.999 for Cx40 and p=1.000 and p=0.998 for Cx43) (Figure 5). To exclude the potential effect of IVC banding on the endothelial Cx expression, the Cx expression in IVC of rats with simple IVC banding without creation of ACF (n=4) was compared with that of sham-operated rats. ICC showed that the patterns of anti-Cx40 and anti-Cx43 labeling in luminal endothelium of IVC of simple IVC-banded rats were identical to those of IVC of sham-operated rats. The anti-Cx37 signal was hardly detectable as found in the sham-operated rats. The GJSNs and TGJAs of Cx40 and Cx43 were similar in both groups (p=0.966 and p=0.951 for Cx 40; p=0.919 and p=0.968 for Cx43) (Figure 6). These findings indicated that the alteration in endothelial Cx expression in IVC-banded ACF rats was not likely to be related to the banding procedure itself.

Discussion

This study investigated the gap junction expression profile in the endothelium of venous vessels exposed to normal venous hemodynamic or increased hemodynamic stresses. We found that the expression of gap junctions in the luminal EC of native vein that is exposed to normal venous hemodynamic stress was generally lower than that of the arteries. Cx37, which was abundantly expressed in the endothelium of thoracic Ao, was hardly detectable in the native IVC. This Cx expression profile was similar to that demonstrated in a previous study done by Inai and Shibata (2009). In the endothelium of rat abdominal IVC, the segment that we observed in this study, they found that the expression level of Cx40 was higher than that of the Cx43 and the level of Cx37 was much less compared with both the Cx40 and Cx43 (Inai and Shibata 2009). Differences in the endothelial phenotype and the hemodynamic conditions between the arteries and veins may be responsible for the differential Cx expression in the endothelium of the arteries and the veins.

When the venous vessels were exposed to a high flow velocity and a mildly but significantly increased pressure by connecting with the artery in the pattern of ACF, the

Figure 4 Representative en face confocal images showing the expression of Cx37, Cx40, and Cx43 in endothelium of the IVC of rats with ACF and rats with IVC-banded ACF (n=4 for each group).

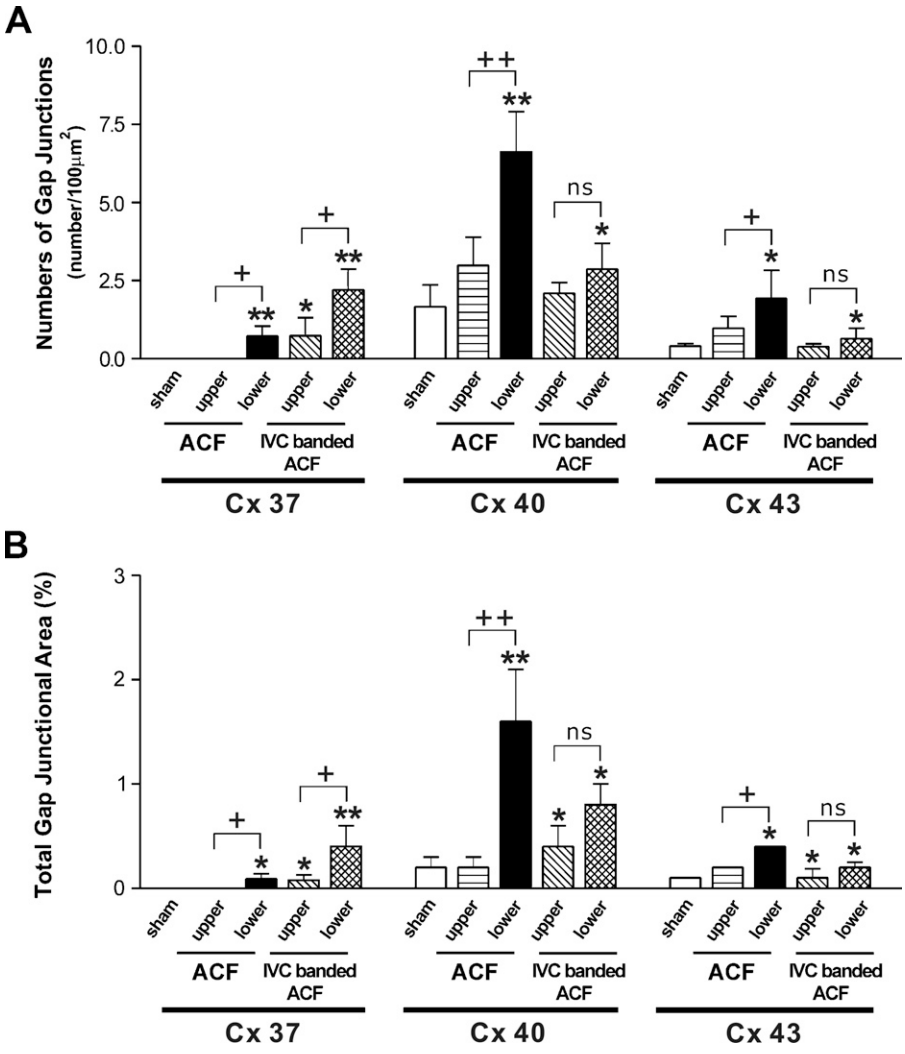

Figure 5 Immunoconfocal analysis of gap junction spots of endothelium of IVC of sham-operated rats, rats with ACF, and rats with IVC-banded ACF (n=4 for each group) detected by antibodies against Cx37, Cx40, and Cx43. (**A**) GJSNs. (**B**) TGJAs. *p<0.05 and **p<0.001 when compared with sham; +p<0.05, ++p<0.001, and nonsignificant (ns) difference when compared between two indicated groups.

Cx37, Cx40, and Cx43 were all markedly upregulated in the endothelium. In this model, the large pressure gradient and the discrepancy of the vascular diameter and elasticity between the Ao and the IVC altogether result in the hemodynamic changes, which have been demonstrated in a previous study to exert a high mean and oscillatory shear stress and increased turbulence intensity to the venous vessels (Sivanesan et al. 1999). Previous studies showed that the increased shear stresses actively regulate the endothelial Cx expressions in cultured cells. Most of those studies focused on Cx43 expression. The effect of increased laminar shear stress on Cx43 expression was controversial. Two studies showed upregulation of Cx43 in cultured endothelial cell in response to sustained levels of increased laminar stress (Cowan et al. 1998; Kwak et al. 2005). However, the level of Cx43 expression was reported to be unchanged in another study (Johnson and Nerem 2007). In contrast to laminar shear stress, oscillatory shear stress has been shown consistently to upregulate endothelial Cx43 (DePaola et al. 1999; Kwak et al. 2005). When the oscillatory shear stress was combined with cyclic circumferential stretch, upregulation of Cx43 was even more prominent (Kwak et al. 2005). In contrast to Cx43, few studies have ever investigated the effect of increased shear stresses on expressions of Cx37 or Cx40. Johnson and Nerem (2007) recently reported that the laminar shear stress upregulated mRNA but not protein of Cx37 or Cx40 in cultured endothelial cells. In ACF model, the endothelial cells of IVC were exposed to a hemodynamic stress that was much more complex than that of the in vitro–cultured cell conditions. Those stresses may synergistically result in upregulation of all three Cxs in the endothelium of IVCs.

In venous vessel exposed to a highly increased pressure and a flow with a mildly increased velocity as in the model of IVC-banded ACF rats, we found that the endothelial Cx40 and Cx43 expression levels remained

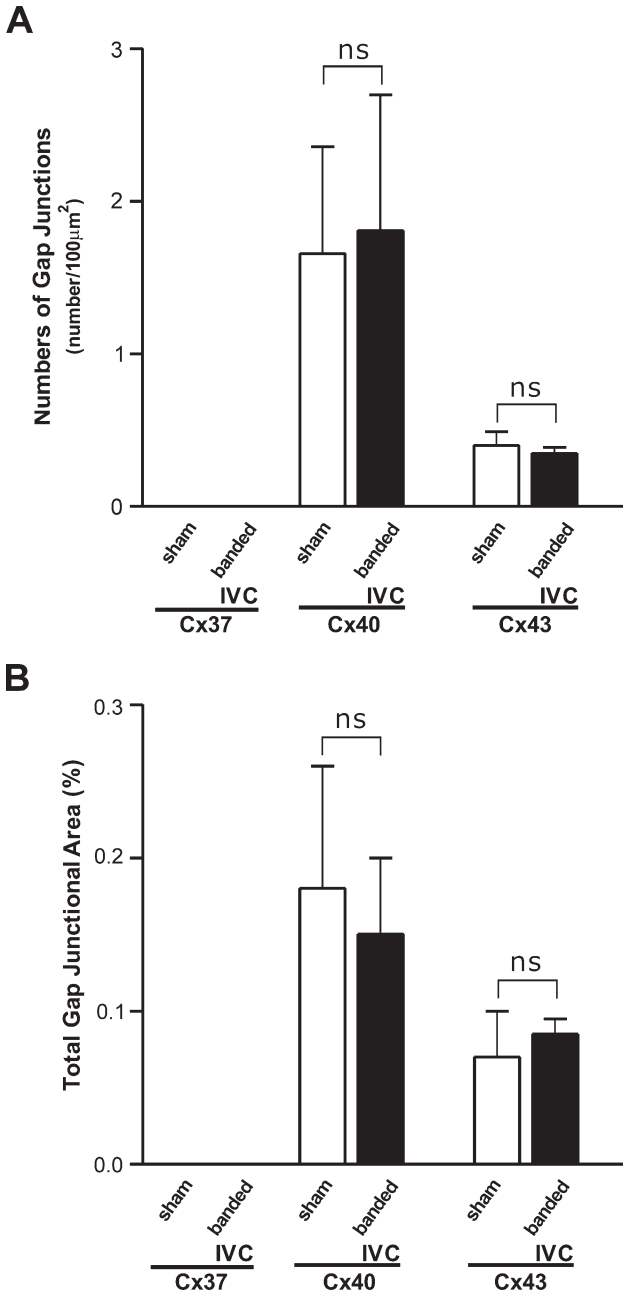

Figure 6 Immunoconfocal analysis of gap junction spots of endothelium of IVC of sham-operated and simple IVC-banded rats, rats with ACF, and rats with IVC-banded ACF (n=4 for each group) detected by antibodies against Cx37, Cx40, and Cx43. (**A**) GJSNs. (**B**) TGJAs. ns, nonsignificant difference when compared between two indicated groups.

similar to those of the native venous vessel. In contrast, the Cx37 was markedly upregulated. This Cx expression profile in response to increased pressure differs from that of the resistant arteries. In the tail artery of spontaneously hypertensive rat, the Cx37, Cx40, and Cx43 were all demonstrated to be downregulated (Rummery et al. 2002). In the mesenteric artery of the same rat model, Kansui et al. (2004) showed that the Cx37 and Cx40 were downregulated and the Cx43, though scarce and heterogenous, was upregulated. In the tail artery of rat with *N*-nitro-L-arginine methyl ester–induced hypertension, Yeh et al. (2006) demonstrated that the endothelial Cx37 and Cx43 were downregulated and the Cx40 remained unchanged. When compared with the resistant arteries, the baseline pressure of the venous vessels before being anastomosed with the arteries is much lower. In addition, the vascular compliance of the venous vessels is much higher than that of the arteries, which may result in a higher circumferential stretch when exposed to an increased pressure. All these factors may potentially contribute to the differences in Cx expressions.

Intercellular communication of endothelial cells through gap junctions has been demonstrated to play a crucial role in regulating vasodilation in arteries and arterioles (de Wit et al. 2000; Figueroa et al. 2003; Mather et al. 2005; Lang et al. 2007). In native venous vessels, the hemodynamic stresses are low and active regulation of the vascular tone may not be mandatory. After being anastomosed with the artery, the venous vessels respond to dramatically increased hemodynamic stresses by acute alteration in vessel tone. Upregulation of endothelial Cxs in vein may play a role in regulating vessel tone to adopt the abrupt hemodynamic changes of the vein grafts.

Recently, Cx43 was shown to play an important role in leukocyte adhesion and transmigration during acute inflammation in vivo (Véliz et al. 2008). In ACF rats, infiltration of neutrophils and monocytes has been found in the vascular walls of vein grafts soon after creation of ACF (Nath et al. 2003). Upregulation of Cx43 in the IVC of ACF rats, as demonstrated in this study, may contribute to the leukocyte infiltration and subsequent development of neointimal hyperplasia.

Limitation

There are several limitations to this study. First, the immunoconfocal study on Cx expression does not provide quantitative data about the absolute amount of a given Cx. However, previous studies have demonstrated that it provides reliable data about the relative expression level of Cx (Green et al. 1993; Blackburn et al. 1995; Yeh et al. 1997). Second, we observed the Cx expression at 1 week after ACF creation. The Cx expression profile may differ between the early and late phases after exposure to the hemodynamic stresses. However, accurate en face observations of the endothelial Cx expression on the whole-mount vein graft tissue using a confocal microscope would be limited by the presence of neointimal tissue at later phase. We have demonstrated recently that neointimal hyperplasia begins to develop in vein graft of ACF rats as early as 2 weeks after creation of the ACF (Chang et al. 2009). The presence of neointimal tissue

would make the tissue surface uneven, which makes en face observation difficult. In addition, the anti-Cx signals that originated from the luminal endothelial cells could not be distinguished from those from smooth muscle cells of the neointima if the neointima is present.

In conclusion, this study shows that the endothelial Cx expression in the venous vessels is generally lower when compared with that in the arteries. When exposed to different hemodynamic models, specific Cx expression pattern was found. The Cx37, Cx40, and Cx43 were all upregulated in endothelium of vein exposed to a highly increased flow velocity and a mildly increased pressure. Only Cx37 was upregulated in the endothelium of vein exposed to a highly increased pressure.

Literature Cited

Blackburn JP, Peters NS, Yeh HI, Rothery S, Green CR, Severs NJ (1995) Upregulation of connexin43 gap junctions during early stages of human coronary atherosclerosis. Arterioscler Thromb Vasc Biol 15:1219–1228

Casey PJ, Dattilo JB, Dai G, Albert JA, Tsukurov OI, Orkin RW, Gertler JP, et al. (2001) The effect of combined arterial hemodynamics on saphenous venous endothelial nitric oxide production. J Vasc Surg 33:1199–1205

Chang CJ, Chen CC, Hsu LA, Chang GJ, Ko YH, Chen CF, Chen MY, et al. (2009) Degradation of the internal elastic laminae in vein grafts of rats with aortocaval fistulae: potential impact on graft vasculopathy. Am J Pathol 174:1837–1846

Cowan DB, Lye SJ, Langille BL (1998) Regulation of vascular connexin43 gene expression by mechanical loads. Circ Res 82: 786–793

DePaola N, Davies PF, Pritchard WF Jr, Florez L, Harbeck N, Polacek DC (1999) Spatial and temporal regulation of gap junction connexin43 in vascular endothelial cells exposed to controlled disturbed flows in vitro. Proc Natl Acad Sci USA 96:3154–3159

De Wit C, Roos F, Bolz SS, Kirchhoff S, Krüger O, Willecke K, Pohl U (2000) Impaired conduction of vasodilation along arterioles in connexin40-deficient mice. Circ Res 86:649–655

Figueroa XF, Paul DL, Simon AM, Goodenough DA, Day KH, Damon DN, Duling BR (2003) Central role of connexin40 in the propagation of electrically activated vasodilation in mouse cremasteric arterioles in vivo. Circ Res 92:793–800

Gabriels JE, Paul DL (1998) Connexin43 is highly localized to sites of disturbed flow in rat aortic endothelium but connexin37 and connexin40 are more uniformly distributed. Circ Res 83:636–643

Green CR, Peters NS, Gourdie RG, Rothery S, Severs NJ (1993) Validation of immunohistochemical quantification in confocal scanning laser microscopy: a comprehensive assessment of gap junction size with confocal and ultrastructural techniques. J Histochem Cytochem 41:1339–1349

Greenfield JC Jr, Rembert JC, Young WG Jr, Oldham HN Jr, Alexander JA, Sabiston DC Jr (1972) Studies of blood flow in aorta-to-coronary venous bypass grafts in man. J Clin Invest 51:2724–2735

Inai T, Shibata Y (2009) Heterogeneous expression of endothelial connexin (Cx) 37, Cx40, and Cx43 in rat large veins. Anat Sci Int 84:237–245

Jiang Z, Berceli SA, Pfahnl CL, Wu L, Goldman D, Tao M, Kagayama M, et al. (2004) Wall shear modulation of cytokines in early vein grafts. J Vasc Surg 40:345–350

Johnson TL, Nerem RM (2007) Endothelial connexin 37, connexin 40, and connexin 43 respond uniquely to substrate and shear stress. Endothelium 14:215–226

Kansui Y, Fujii K, Nakamura K, Goto K, Oniki H, Abe I, Shibata Y, et al. (2004) Angiotensin II receptor blockade corrects altered expression of gap junctions in vascular endothelial cells from hypertensive rats. Am J Physiol Heart Circ Physiol 287:H216–224

Kwak BR, Silacci P, Stergiopulos N, Hayoz D, Meda P (2005) Shear stress and cyclic circumferential stretch, but not pressure, alter connexin43 expression in endothelial cells. Cell Commun Adhes 12:261–270

Lang NN, Luksha L, Newby DE, Kublickiene K (2007) Connexin 43 mediates endothelium-derived hyperpolarizing factor-induced vasodilatation in subcutaneous resistance arteries from healthy pregnant women. Am J Physiol Heart Circ Physiol 292:H1026–1032

Mather S, Dora KA, Sandow SL, Winter P, Garland CJ (2005) Rapid endothelial cell-selective loading of connexin 40 antibody blocks endothelium-derived hyperpolarizing factor dilation in rat small mesenteric arteries. Circ Res 97:399–407

Nath KA, Kanakiriya SKR, Grande JP, Croatt AJ, Katusic ZS (2003) Increased venous proinflammatory gene expression and intimal hyperplasia in an aorto-caval fistula model in the rat. Am J Pathol 162:2079–2090

Rummery NM, McKenzie KU, Whitworth JA, Hill CE (2002) Decreased endothelial size and connexin expression in rat caudal arteries during hypertension. J Hypertens 20:247–253

Sivanesan S, How TV, Black RA, Bakran A (1999) Flow patterns in the radiocephalic arteriovenous fistula: an in vitro study. J Biomech 32:915–925

Spray TL, Roberts WC (1976) Tension on coronary bypass conduits. A neglected cause of real or potential obstruction of saphenous vein grafts. J Thorac Cardiovasc Surg 72:282–287

Van Rijen H, van Kempen MJ, Analbers LJ, Rook MB, van Ginneken AC, Gros D, Jongsma HJ (1997) Gap junctions in human umbilical cord endothelial cells contain multiple connexins. Am J Physiol 272(1 Pt 1):C117–130

Véliz LP, González FG, Duling BR, Sáez JC, Boric MP (2008) Functional role of gap junctions in cytokine-induced leukocyte adhesion to endothelium in vivo. Am J Physiol Heart Circ Physiol 295: H1056–1066

Wang LC, Guo GX, Tu R, Hwang NH (1990) Graft compliance and anastomotic flow patterns. ASAIO Trans 36:90–94

Yeh HI, Chang HM, Lu WW, Lee YN, Ko YS, Severs NJ, Tsai CH (2000) Age-related alteration of gap junction distribution and connexin expression in rat aortic endothelium. J Histochem Cytochem 48:1377–1389

Yeh HI, Lai YJ, Lee YN, Chen YJ, Chen YC, Chen CC, Chen SA, et al. (2003) Differential expression of connexin43 gap junctions in cardiomyocytes isolated from canine thoracic veins. J Histochem Cytochem 51:259–266

Yeh HI, Lee PY, Su CH, Tian TY, Ko YS, Tsai CH (2006) Reduced expression of endothelial connexins 43 and 37 in hypertensive rats is rectified after 7-day carvedilol treatment. Am J Hypertens 19:129–135

Yeh HI, Lupu F, Dupont E, Severs NJ (1997) Upregulation of connexin43 gap junctions between smooth muscle cells after balloon catheter injury in the rat carotid artery. Arterioscler Thromb Vasc Biol 17:3174–3184

Yeh HI, Rothery S, Dupont E, Coppen SR, Severs NJ (1998) Individual gap junction plaques contain multiple connexins in arterial endothelium. Circ Res 83:1248–1263

The Journal of Histochemistry & Cytochemistry